Published in final edited form as:
Biochem Pharmacol. 2013 March 15; 85(6): 808–816. doi:10.1016/j.bcp.2012.12.003.

A p21-activated kinase (PAK1) signaling cascade coordinately regulates F-actin remodeling and insulin granule exocytosis in pancreatic β cells

Michael A. Kalwat[1,*], **Stephanie M. Yoder**[2], **Zhanxiang Wang**[2], and **Debbie C. Thurmond**[1,2,3,†]

[1]Department of Biochemistry and Molecular Biology, Indiana University School of Medicine, Indianapolis, IN, USA

[2]Herman B Wells Center for Pediatric Research, Basic Diabetes Group, Department of Pediatrics, Indiana University School of Medicine, Indianapolis, IN, USA

[3]Department of Cellular and Integrative Physiology, Indiana University School of Medicine, Indianapolis, IN, USA

Abstract

Human islet studies implicate an important signaling role for the Cdc42 effector protein p21-activated kinase (PAK1) in the sustained/second-phase of insulin secretion. Because human islets from type 2 diabetic donors lack ~80% of normal PAK1 protein levels, the mechanistic requirement for PAK1 signaling in islet function was interrogated. Similar to MIN6 β cells, human islets elicited glucose-stimulated PAK1 activation that was sensitive to the PAK1 inhibitor, IPA3. Given that sustained insulin secretion has been correlated with glucose-induced filamentous actin (F-actin) remodeling, we tested the hypothesis that a Cdc42-activated PAK1 signaling cascade is required to elicit F-actin remodeling to mobilize granules to the cell surface. Live-cell imaging captured the glucose-induced cortical F-actin remodeling in MIN6 β cells; IPA3-mediated inhibition of PAK1 abolished this remodeling. IPA3 also ablated glucose-stimulated insulin granule accumulation at the plasma membrane, consistent with its role in sustained/second-phase insulin release. Both IPA3 and a selective inhibitor of the Cdc42 GTPase, ML-141, blunted the glucose-stimulated activation of Raf-1, suggesting Raf-1 to be downstream of Cdc42→PAK1. IPA3 also inhibited MEK1/2 activation, implicating the MEK1/2→ERK1/2 cascade to occur downstream of PAK1. Importantly, PD0325901, a new selective inhibitor of MEK1/2→ERK1/2 activation, impaired F-actin remodeling and the sustained/amplification pathway of insulin release. Taken together, these data suggest that glucose-mediated activation of Cdc42 leads to activation of PAK1 and prompts activation of its downstream targets Raf-1, MEK1/2 and ERK1/2 to elicit F-actin remodeling and recruitment of insulin granules to the plasma membrane to support the sustained phase of insulin release.

†To whom correspondence should be addressed: Debbie C. Thurmond, PhD. 635 Barnhill Dr., MS2031, Herman B Wells Center for Pediatric Research, Department of Pediatrics, Indianapolis, IN 46202. Tel: 317-274-1551; Fax. 317-274-4107; dthurmon@iupui.edu.
*present address: Department of Pharmacology, University of Texas Southwestern Medical Center, Dallas, TX, USA

Keywords

insulin granule; exocytosis; Cdc42; F-actin remodeling; islet β cell; PAK1

1. Introduction

Insulin is secreted from pancreatic β cells in a biphasic manner in response to fuel secretagogues. A first-phase peak in secretion occurs within 10 minutes after glucose stimulation. Following first phase, a lower-rate sustained second-phase secretion occurs that can persist for hours (1). Biphasic insulin secretion occurs when glucose enters the β cell through GLUT2 glucose transporters and is metabolized leading to an increased ATP:ADP ratio (1). This leads to the inhibition of ATP-sensitive K^+ channels, causing membrane depolarization and calcium influx through voltage-sensitive calcium channels which results in fusion of insulin granules juxtaposed to the plasma membrane (2-5). Second phase secretion is presumed to require granule mobilization from more distant storage pools of insulin granules that may restricted from reaching the plasma membrane. A substantial body of evidence suggests that stimulation of the β cell with glucose yields dynamic disruptions in cortical filamentous actin (F-actin) that may facilitate insulin granule mobilization to the cell surface (6-13); such diminished F-actin intensity or fragmentation of the cortical ring of F-actin is defined as cortical F-actin remodeling (9). Glucose-induced cortical F-actin remodeling becomes visible during the first phase of insulin release (7, 9, 12, 14). It has been predicted that factors produced/activated in response to this glucose stimulation transmit the signal(s) to amplify and sustain insulin secretion beyond the first phase (15).

Cdc42 has been suggested as an amplification signal given its key and proximal role leading to second-phase glucose-stimulated insulin secretion; depletion or inactivation of Cdc42 from human or rodent islets selectively impairs the second-phase (16, 17). Multiple studies have shown that upon entry of stimulatory levels of glucose into the β cell, Cdc42 is activated within ~3 min (14, 17-19), during the time of the first-phase of insulin release. Activated Cdc42 binds to its downstream effector, p21-activated kinase (PAK1), which in turn induces PAK1 phosphorylation and activation. Like Cdc42, PAK1 is similarly required for second-phase insulin release (16, 17). Activation of Rac1, a small GTPase implicated both in F-actin changes and in insulin release, requires Cdc42 and PAK1 to become activated (17). However, Rac1 activation occurs more than 10 min after the initiation of F-actin remodeling or that of second-phase insulin release in β cells (17, 20, 21).

In considering alternative means by which the glucose signal is propagated to evoke F-actin remodeling, PAK1 is known to utilize multiple substrates with the potential to elicit changes in F-actin structure, including LIMK (22), Filamin A (23), p41-Arc (24), MLCK-MLC pathways (25), and the MAPK pathway through Raf/MEK1/2 (26, 27). However, recent studies of islets from PAK1 knockout mice suggest against a required role for LIMK in cofilin phosphorylation, and instead point to a role in ERK activation (16). Whether PAK1 signaling or PAK1 scaffolding leads to ERK activation remains untested, as does the role of either protein in glucose-stimulated cortical F-actin remodeling in β cells.

PAK1 is implicated in type 2 diabetes, since islets from type 2 diabetic individuals contain 80% less PAK1 protein than non-diabetic individuals (16). Moreover, PAK1 is located in a region of chromosome 11 that is linked to type 2 diabetes disease risk (28, 29), adding the potential for PAK1 gene variants to contribute to disease. Therefore, determining how PAK1 functions in regulating insulin secretory processes in islet β cells may provide insight into why defects in PAK1 are linked to diabetes or diabetic susceptibility.

In this study, using new inhibitors against Cdc42 activation, PAK1 activation, and a new more selective inhibitor of MEK1/2, we derived the following pathway required for glucose-induced F-actin remodeling using both human and rodent islet β cells: Cdc42→PAK1→Raf-1-MEK1/2→ERK1/2. Moreover, we present evidence to suggest that this signaling cascade induces glucose-induced F-actin remodeling to facilitate the recruitment/accumulation of insulin granules to the plasma membrane to support the sustained/second phase of insulin.

2. Materials and Methods

2.1 Materials

Rhodamine-Phalloidin was from Life Technologies (Grand Island, NY). Latrunculin B was from Calbiochem (Billerica, MA). Rabbit anti-phospho-ERK1/2, mouse anti-ERK1/2, rabbit anti-phospho-MEK1/2, rabbit anti-MEK1/2, and rabbit anti-PAK1 antibodies were from Cell Signaling Technology (Danvers, MA). Diazoxide, IPA3, and rabbit anti-phospho-PAK1 (Thr423) antibody was purchased from Santa Cruz (Santa Cruz, CA). Mouse anti-SNAP-25, anti-VAMP2 and rabbit anti-actin antibodies were purchased from BD Biosciences (Mountain View, CA), Synaptic Systems (Germany), and Sigma (St. Louis, MO), respectively. Goat anti-mouse horseradish peroxidase secondary antibody and PD0325901 were obtained from Thermo Fisher Scientific (Rockford, IL). Goat anti-rabbit horseradish peroxidase secondary antibody and TransFectin™ lipid reagent were acquired from Bio-Rad (Hercules, CA). ECL reagent and SuperSignal™ Femto were purchased from GE Healthcare (Piscataway, NJ) and Pierce (Rockford, IL), respectively. The rat insulin radioimmunoassay kits were obtained from Millipore (Billerica, MA). The Lifeact-GFP plasmid was kindly provided by Dr. Louis Philipson (University of Chicago, (30)). The ML-141 inhibitor was kindly provided by the KU Specialized Chemistry Center (University of Kansas, Lawrence, KS). The F/G Actin ratio kit was obtained from Cytoskeleton (Denver, CO). All other chemicals were obtained through Thermo Fisher Scientific or Sigma.

2.2 Cell culture, transient transfection, and secretion assays

MIN6 β cells (gift from Dr. John Hutton, University of Colorado Health Sciences Center, Denver, CO) were cultured in Dulbecco's modified Eagle's medium (25 mM glucose), supplemented with 15% fetal bovine serum, 100 units/ml penicillin, 100 μg/ml streptomycin, 292 μg/ml L-glutamine, and 50 μM β-mercaptoethanol as described previously (31). MIN6 cells were transfected with TransFectin™ (Bio-Rad) according to the manufacturer's instructions and cultured 48 h before use in experiments. For experiments where cells were starved and stimulated, MIN6 cells were washed twice with and incubated for 2 h in freshly prepared modified Krebs-Ringer bicarbonate buffer (MKRBB: 5 mM KCl, 120 mM NaCl, 15 mM HEPES, pH 7.4, 24 mM $NaHCO_3$, 1 mM MgCl2, 2 mM $CaCl_2$, and 1 mg/ml radioimmunoassay-grade BSA). Cells were stimulated with 20 mM glucose as indicated and insulin secreted into the buffer was quantified using a rat insulin radioimmunoassay kit. Cells were lysed in 1% Nonidet P-40 (NP-40) lysis buffer (25 mM HEPES, pH 7.4, 1% Nonidet P-40, 10% glycerol, 50 mM sodium fluoride, 10 mM sodium pyrophosphate, 137 mM NaCl, 1 mM sodium vanadate, 1 mM phenylmethylsulfonyl fluoride, 10 μg/ml aprotinin, 1 μg/ml pepstatin, 5 μg/ml leupeptin) and cleared of insoluble material by centrifugation for 10 min at 4°C for subsequent use in co-immunoprecipitation experiments.

2.3 Subcellular fractionation

As described previously (18), all fractionation steps were performed at 4°C. Briefly, MIN6 cells at 70-80% confluence were harvested into 1 ml of homogenization buffer (20 mM Tris-HCl, pH 7.4, 0.5 mM EDTA, 0.5 mM EGTA, 250 mM sucrose, 1 mM dithiothreitol, 100

μM phenylmethylsulfonyl fluoride, 4 μg/ml aprotinin, 2 μg/ml pepstatin, and 10 μg/ml leupeptin). Cells were homogenized by 10 strokes through a 27-gauge needle, and then centrifuged at 900 × g for 10 min. Post-nuclear supernatants were centrifuged for 5500 × g for 15 min. The resulting supernatant was centrifuged at 25,000 × g for 20 min to obtain the secretory granule fraction in the pellet. The plasma membrane (PM) fraction was prepared by mixing the post-nuclear pellet with 1 volume of Buffer A (0.25 M sucrose, 1 mM $MgCl_2$, and 10 mM Tris-HCl, pH 7.4) and 2 volumes of Buffer B (2 M sucrose, 1 mM $MgCl_2$, 10 mM Tris-HCl, pH 7.4). This mixture was overlaid with Buffer A and centrifuged at 113,000 × g for 1 h to obtain an interface containing the PM. The interface was collected, diluted to 1.5 ml with homogenization buffer, and centrifuged at 6000 × g for 10 min. The resulting pellet contained the PM fraction. All collected pellets were resuspended in 1% NP-40 lysis buffer.

2.4 Co-immunoprecipitation and immunoblotting

For immunoprecipitation, 2-3 mg of cleared detergent lysate protein was combined with 1 μg of antibody per mg protein and the reaction rotated for 2 h at 4°C. Protein G Plus agarose beads (Santa Cruz) were added and reactions rotated at 4°C for an additional 2 h. Beads were pelleted and washed three times with lysis buffer and resulting immunoprecipitates were resolved on 10-12% SDS-PAGE and transfer to PVDF membranes for immunoblotting. Immunoreactive bands were visualized with ECL, ECL Prime (GE Healthcare, Piscataway, NJ), or Supersignal Femto (Pierce) reagents and imaged using a Chemi-Doc gel documentation system (Bio-Rad, Hercules, CA). Phosphorylated and total ERK1/2 blots were visualized using goat anti-mouse 680 and goat anti-rabbit 800 simultaneously and imaged on a Licor imaging system.

2.5 Confocal microscopy

MIN6 cells plated onto glass coverslips at 30% confluence were transiently transfected with 4 μg of Life-Act-GFP plasmid DNA/35 mm well. After 48 h incubation, cells were placed in MKRBB for 2 h, followed by stimulation with 20 mM glucose for 5 min and then immediately fixed and permeabilized in fixation/permeabilization buffer (4% paraformaldehyde, 0.1% Triton X-100 at 4°C) for 10 min in the dark. Fixed and permeabilized cells were blocked (1% BSA plus 5% donkey serum in PBS) for 1 h at room temperature, followed by incubation with 0.17 μM Rhodamine-Phalloidin for 1 h. Cells were washed three times with PBS and during the final wash, DAPI was added to stain nuclei. All cells were washed again with PBS, and mounted (using Vectashield) for confocal microscopy. Fluorescent cells were imaged using single-channel scanning with a 60X objective (2X zoom) using an Olympus FV1000-MPE confocal microscope (Olympus, Center Valley, PA). To score F-actin remodeling, only cells on the outside of clusters were counted. Cells with discontinuous cortical F-actin after 5 min of glucose stimulation were scored as exhibiting F-actin remodeling. At least 100 cells were counted for each condition in the experiments for Figure 5.

2.6 Live-cell imaging

MIN6 cells were plated on 35 mm glass-bottom MatTek culture dishes (MatTek), grown to 30-50% confluency and transfected with Lifeact-GFP. Forty-eight h later cells were incubated in MKRBB containing either 1 μl DMSO (vehicle) or inhibitors as stated in figure legends. For confocal live-cell imaging, cells were constantly perfused with MKRBB containing DMSO or IPA3 and imaged on an Olympus FV1000-MPE. For each condition, 11 cells were analyzed for F-actin remodeling across three independent experiments. For Apotome™ live-cell imaging data was collected using a Zeiss Axio Observer™ with a Plan-Apochromat 63X objective equipped with a Hamamastu Orca-ER digital camera and an Apotome™ and analyzed using ImageJ software (NIH).

2.7 Human islet culture

Pancreatic human islets were obtained through the Integrated Islet Distribution Program, IIDP. Criteria for human donor islet acceptance: receipt within 36 h of isolation, and of at least 70% purity and 75% viability. Upon receipt, human islets were first allowed to recover in CMRL medium for 2 h, and then were handpicked using a green gelatin filter to eliminate residual non-islet material. Human islets were cultured overnight in CMRL containing either DMSO or IPA3 (7.5 μM) prior to glucose time course experiments: 100-200 islets were preincubated for 1 h in KRBH buffer plus DMSO or IPA3 (10 mM HEPES pH 7.4, 134 mM NaCl, 5 mM $NaHCO_3$, 4.8 mM KCl, 1 mM $CaCl_2$, 1.2 mM $MgSO_4$, 1.2 mM KH_2PO_4 containing 0.5 mg/ml BSA) supplemented with 2.8 mM glucose. Islets were then stimulated for the times stated in figure legends with 16.7 mM glucose, washed in cold PBS, and lysed and boiled in Laemmli sample buffer for SDS-PAGE protein resolution and immunoblot analysis.

2.8 Statistical analysis

All data were evaluated for statistical significance using Student's *t* test. Data are expressed as the average ± SE. One-way ANOVA was performed using GraphPad Prism™ software (La Jolla, CA).

3. Results

3.1 PAK1 activation in human islets is prevented by IPA3

While it has been shown that PAK1 activation occurs in human islets and is dependent on upstream glucose-stimulated Cdc42 activation (16), whether the time course of activation in human islets mimics that observed in mouse clonal β cells was unknown. Toward this, three independent batches of human cadaveric islets from non-diabetic donors were obtained and left either unstimulated or were stimulated with 16.7 mM glucose for 5 or 10 minutes and assessed for relative levels of phosphorylated $PAK1^{Thr423}$/total PAK1 content by immunoblot analysis. Similar to the clonal MIN6 β cells, PAK1 phosphorylation was increased by 1.9-fold within 5 min of glucose stimulation (Figure 1A) (pPAK/PAK for 5 min glucose=1.9 ± 0.6 and for 10 min glucose=1.4 ± 0.1 fold over basal, $P<0.05$). ERK1/2 phosphorylation served as an indicator of islet responsiveness to glucose, showing a ~3-fold increase (Figure 1A) (pERK/ERK for 5 min glucose=3.1 ± 0.8 and for 10 min glucose=2.7 ± 0.6 fold over basal, $P<0.05$). Furthermore, human islets treated with the PAK1 inhibitor IPA3, as described previously (16), exhibited reduced PAK1 activation ($PAK1^{Thr423}$/total PAK1 content) in response to glucose stimulation (Figure 1B) (pPAK/PAK for IPA3=0.8 ± 0.1, compared to DMSO set equal to1.0). IPA3 inhibits the activation of PAK1 selectively in response to the small GTPase Cdc42 (32, 33). These data validated the use of IPA3 as a tool to study the role of the Cdc42-PAK1 activation pathway in β cells, as well as the suitability of the MIN6 β cells as an appropriate model system for mechanistic studies pertaining to PAK1 function.

3.2 PAK1 activity is necessary for glucose-induced cortical F-actin remodeling

Cdc42 cycling has been implicated as an upstream signal to trigger F-actin remodeling in β cells (34). To determine whether the activation of PAK1, the effector of Cdc42 in β cells, is required for glucose-induced cortical F-actin remodeling, MIN6 cells were acutely treated with or without IPA3 and F-actin remodeling assessed by live-cell confocal microscopy. Changes in cortical F-actin were captured using the Lifeact-GFP biosensor (35). Lifeact is a 17 residue peptide from the actin binding protein Abp140, and when linked to the N-terminus of GFP to form Lifeact-GFP, has been shown to bind specifically to F-actin in live β cells without adversely affecting F-actin dynamics (30, 36). Live-cell imaging of vehicle-

treated (DMSO) cells expressing Lifeact-GFP captured the first visible changes in the cortical F-actin to occur at 5 min after glucose stimulation (Figure 2A, left panels) (80% of cells exhibited remodeling), consistent with prior reports using cells fixed after 5 min of glucose stimulation and F-actin visualized using the selective F-actin binding agent phalloidin (9, 12, 13). In contrast, acute preincubation of MIN6 cells (10 min) with the PAK1 inhibitor IPA3 prior to glucose stimulation fully abolished the effect of glucose upon F-actin remodeling (Figure 2A, right panels) (0% of cells exhibited remodeling). Treatment with IPA3 had no impact on the cellular F:G-actin ratio under either basal (Figure 2B) or glucose-stimulated conditions (F:G-actin ratio: DMSO, 10:90 ± 3% *versus* IPA3-treated, 10:90 ± 2%, n=3; $p>0.05$), indicating that the blunting effect of IPA3 upon glucose-induced F-actin remodeling was not due to increased levels of cellular F-actin.

3.3 Cdc42-PAK1 signals to Raf-1 and MEK1/2 in response to glucose

We previously showed that knockdown or knockout of PAK1 resulted in selectively decreased ERK1/2 activation (16), although it remained possible that these more chronic approaches could be coupled to a need for PAK1's functions in protein scaffolding. Having established IPA3 as an acute approach to inactivate but not deplete PAK1, we next determined whether PAK1 signaled through the Raf-1 and/or MEK1/2 en route to ERK1/2, proteins previously implicated in insulin secretion (37, 38). Indeed, glucose induced a significant 1.6-fold increase in Raf-1^{S338} phosphorylation in vehicle-treated (DMSO) MIN6 cells, whereas preincubation with IPA3 for 10 min fully ablated this increase (Figure 3A). The role of Cdc42 as an upstream activator of PAK1 signaling in this pathway was supported by studies showing that pretreatment with the Cdc42 inhibitor ML-141 (39) similarly abolished the glucose-induced increase in pRaf-1^{S338} (Figure 3B). MEK1/2, a canonical target of Raf kinase, is known to be downstream of PAK1 in other systems (27). In MIN6 cells, MEK1/2 was found to undergo glucose-stimulated phosphorylation on Ser 217/221 at 5 min (Figure 3C): (pMEK/MEK for 5 min glucose=3.1 ± 1.7 fold over basal). In contrast, acute pretreatment with IPA3 significantly reduced glucose-stimulated MEK1/2 phosphorylation, suggesting PAK1 signaling to be important for MEK1/2 activation in β cells (Figure 3D) (pMEK/MEK for IPA3=0.6 ± 0.1 compared to DMSO set equal to 1.0, $P<0.05$). IPA3 treatment similarly attenuated glucose-stimulated MEK1/2 phosphorylation in two independent batches of human islets (data not shown). These data demonstrate that PAK1 is necessary for MEK1/2 activation in both human islets and MIN6 cells.

3.4 ERK1/2 signaling contributes to the amplifying/sustained phase of insulin secretion and cortical F-actin remodeling

We next questioned whether PAK1 signaling through MEK1/2 is required for ERK1/2 signaling, and if this underlies the requirement for PAK1 in glucose-stimulated insulin secretion. To test this, we quantified insulin secretion from MIN6 cells treated with the MEK1/2 inhibitor, PD0325901 (hereafter referred to as 'PD03'). PD03 has a much lower IC_{50} than its predecessor MEK1/2 inhibitors PD98059 or U0126, and has very little activity against kinases other than MEK1/2, allowing its use at lower concentrations that reduce the risk of off-target effects (40). Low dosage PD03 treatment was found to block ERK1/2 phosphorylation/activation (Figure 4A), confirming that ERK1/2 activation lies downstream of MEK1/2 in the MIN6 β cells. This correlated with a 30% reduction in glucose-stimulated insulin secretion after 30 min of stimulation (Figure 4B). Since 30 min of glucose stimulation will encompass insulin release during both phases of secretion, we also employed the diazoxide paradigm in effort to selectively examine the requirement for ERK1/2 in the amplifying/sustained phase of insulin secretion. In addition, the use of MIN6 β cells for these studies eliminates the possible effects of MEK inhibition on non-β cell types of the islet. The diazoxide paradigm is based upon the premise that the triggering/first-phase release is due to an ATP-sensitive potassium channel (K_{ATP})-dependent pathway,

while the sustained/second-phase/amplifying pathway of insulin secretion is largely regulated by K_{ATP} channel-independent effects (41-44). When β cells are depolarized with KCl in the presence of the K_{ATP} channel opener diazoxide, the triggering phase is stimulated, while the further addition of glucose simulates the amplifying phase. MIN6 cells were pretreated with either vehicle (DMSO) or PD03 for 1 h, followed by addition of diazoxide for 10 min before stimulation with 30 mM KCl or 30 mM KCl plus 20 mM glucose. While vehicle-treated cells showed a robust 4-fold amplification response to the addition of glucose during the 30 min stimulation period, PD03-treated cells showed significantly reduced glucose-amplified insulin secretion (Figure 4C). PD03-treated cells showed no significant decrease in the triggering response (Dz+KCl only). These data suggest that glucose-induced ERK activation is required for the amplifying/second-phase of insulin release. This finding reiterated the selective effect of IPA3 upon second-phase insulin release (16).

Given the requirement for PAK1 signaling in glucose-stimulated F-actin remodeling, and the known relationship between sustained insulin release and F-actin remodeling, we next investigated the potential coupling through MEK1/2-ERK1/2 signaling in this process. MIN6 cells were pretreated with vehicle (DMSO) or PD03 followed by 5 min of stimulation with glucose, and fixed and stained with phalloidin for quantification of F-actin remodeling by confocal microscopy. IPA3-treated cells served as a control for detection of blunted glucose-induced cortical F-actin remodeling. While ~40% of vehicle-treated cells exhibited remodeling of F-actin after 5 min of glucose stimulation, the occurrence of F-actin remodeling in PD03-treated cells was significantly reduced (Figure 5). These data point to a need for glucose-stimulated PAK1 signaling through MEK1/2 and ERK1/2 to evoke F-actin remodeling, correlated with insulin release.

3.5 PAK1 activity is required for glucose-induced insulin granule accumulation at the plasma membrane

Glucose-induced PAK1 activation and its role in inducing F-actin remodeling may be required for granule recruitment/mobilization to promote the accumulation of insulin granules at the PM. To test this, MIN6 cells treated acutely with IPA3 versus vehicle were subjected to subcellular fractionation to separate PM-localized granules from intracellular storage granule (SG)-pools, and the abundance of PM-localized granules quantified under basal and glucose-stimulated conditions. VAMP2 is the v-SNARE protein present on the insulin granule and known to be required for SNARE-mediated insulin exocytosis (45), and therefore serves as a marker of insulin granule locale within the β cell. This method recapitulates granule localization linked to cytoskeletal changes as determined by electron microscopy, and thus was employed here. Compared to unstimulated cells, the ratio of VAMP2 present in the PM and SG fractions was significantly increased by ~40% after 20 min of glucose-stimulation (Figure 6), as described (34). However, IPA3-treated cells stimulated with glucose exhibited no increase in VAMP2 at the PM (Figure 6). These data suggested that PAK1 activity may be required for glucose-induced insulin granule recruitment to and/or retention/capture at the PM.

4. Discussion

In the current study, we demonstrate for the first time that Cdc42→PAK1 signaling is essential to F-actin cytoskeletal remodeling to facilitate glucose-stimulated insulin secretion. Furthermore, we mapped the first signaling itinerary downstream of the proximal Cdc42→PAK1 activation step in the islet β cell required for evoking this F-actin remodeling: PAK1→Raf-1-MEK1/2→ERK1/2. Moreover, the distal step was shown to be important for the sustained/amplification phase of glucose-stimulated insulin release,

corroborating previous reports of Cdc42-PAK1 importance in this phase (16, 17). Coordinate with showing PAK1→MEK1/2→ERK1/2 signaling to be critical for normal glucose-induced F-actin remodeling, PAK1 signaling was also required for insulin granule accumulation at the PM. Taken together, these data prompt a new mechanistic model to describe how Cdc42-PAK1 signaling is linked to second-phase insulin release: *1)* glucose activates a Cdc42-PAK1 signaling pathway to subsequently activate Raf-1, MEK1/2 and ERK1/2, to *2)* induce F-actin remodeling, which *3)* yields a net increase of insulin granules at the PM necessary to sustain exocytosis during the second/amplification phase of insulin release (Figure 7).

Data herein are the first to point to PAK1→MEK1/2 signaling as a major pathway accounting for glucose-induced cortical F-actin remodeling in the β cell. Consistent with our findings, ERK1/2 activation is reportedly blunted in a β cell line known to be refractory to glucose-induced actin remodeling (11). Interestingly, in normal glucose-responsive β cells, activated ERK1/2 was shown to be localized to the tips of actin filaments (11), placing it in the proper locale to act upon proteins involved in F-actin remodeling and insulin granule trafficking/exocytosis. However, since our PD03-treated cells retained some remodeling, more so than did the IPA3-treated cells, we must also consider alternate PAK1 targets. Although we have already shown PAK1 to be dispensable for β cell cofilin phosphorylation (16), known to occur via PAK1-LIM kinase activation (22), PAK1 signaling to Filamin A or MLCK-myosin regulatory light chain 2 (MLC2) must also be considered. For example, PAK1 phosphorylates Filamin $A^{Ser2152}$, and the phosphorylated form of Filamin A has been linked to its action in F-actin dynamics in other cell types (23, 46). PAK1 also targets MLCK, which then phosphorylates MLC2 to promote actin remodeling processes in other cell systems (47). Phosphorylated MLC has been reported in MIN6 β cells (48) with MLC2 phosphorylation at Ser19 induced in response to glucose stimulation (49, 50). Alternatively, ERK1/2 has been shown to signal to MLCK in other cell types (51), and thus it remains possible that PAK1 could signal through MLCK/MLC2 via ERK1/2. Experiments are underway to determine the relative importance of PAK1 signaling to MLCK-MLC2 for glucose-induced actin remodeling.

Having placed ERK1/2 at the distal end of the signaling pathway leading to F-actin remodeling concomitant with a role in the amplification/sustained phase of insulin release, our results are supportive of a growing body of evidence. For example, a number of studies favoring a role for ERK1/2 in sustained-phase insulin release stem from experimentation using siRNA-mediated knockdown of ERK1/2 and Raf/MEK1/2 inhibitor treatments in β cells (37, 52, 53). However, contradictory data do exist, such as an earlier report arguing that ERK1/2 plays only a mitogenic role in β cells (54). At the time of that report the MEK1/2 inhibitor available was PD98059, now recognized as being less efficient and less selective than PD03, and thus may have contributed to the controversy. Using PD03 acutely in the present study, we found no evidence of alterations in insulin content in islet β cells (data not shown), suggesting that expression of insulin at the protein level was not impacted by the short-term block in ERK1/2 activation. In addition, studies using PD98059 post conflicting data regarding its role in early versus later phase secretion, although both did not assess using islet perifusion (11, 52). As with the study using PD98059 in perifused islets (52), our data using PD03 in the diazoxide paradigm indicate the primary role of ERK1/2 to be in the later phase.

In addition to functioning in glucose-induced F-actin remodeling and second-phase insulin release, PAK1 has recently been shown to be a substrate of the SAD-A kinase (55), although it remains to be determined if this is also dependent upon Cdc42. SAD-A kinase is activated downstream of cAMP (55). cAMP levels are elevated in the β cell via GLP-1 binding to the GLP-1 receptor. Upon activation of the GLP-1 receptor, adenylyl cyclase is activated and

produces cAMP, and this in turn activates both PKA and Epac2 (56). PKA inhibitors have been shown to prevent glucose stimulated ERK1/2 activation (52, 57), and multiple stimuli (GLP-1, forskolin) that increase cAMP levels in β cells also potentiate ERK1/2 activation (57, 58). Now knowing the importance of PAK1 in cortical F-actin remodeling in the β cell, future studies will be required to determine the linkage between Cdc42-PAK1, cAMP-PKA, and ERK1/2 signaling in evoking F-actin remodeling to support glucose-stimulated and GLP-1-augmented second-phase insulin secretion. Since signaling through both PAK1 and cAMP-PKA can act in second-phase insulin secretion, it is tempting to speculate that PAK1 may play a role in mediating GLP-1 action.

In summary, we showed that PAK1 signals to the Raf-1-MEK1/2-ERK1/2 in β cells and that MEK1/2-ERK1/2 signaling is necessary for normal glucose-induced insulin secretion and F-actin remodeling. We also determined that PAK1 is required for glucose-stimulated F-actin remodeling and insulin granule accumulation in plasma membrane fractions, implicating the Cdc42-PAK1 signaling pathway in granule mobilization to support the sustained release of insulin. In addition, these results have implications in other secretory cell systems relevant to type 2 diabetes where PAK1 may play a vital role, such as GLP-1 secretion from enteroendocrine L cells of the gut (59), and insulin-stimulated glucose uptake into skeletal muscle cells (16, 17). As such, it is clear that specifically enhancing PAK1 signaling in certain tissues has potential as a strategy for therapeutic intervention for type 2 diabetes. However, we must be mindful that PAK1 protein levels are significantly decreased in type 2 diabetic human islets, such that treatments that act through the Cdc42-PAK1 pathway may not be effective unless PAK1 levels are first restored.

Acknowledgments

We are grateful to the KU Specialized Chemistry Center (University of Kansas, Lawrence, KS) for supplying us with the ML-141 material, and to Dr. Louis Philipson for sharing the Lifeact-GFP plasmid (University of Chicago, Chicago, IL). We would also like to thank Drs. Raghu Mirmira, D. Wade Clapp, Patrick Fueger, Eunjin Oh and Dean Wiseman, and Latha Ramalingam and Yichun Chen for many helpful discussions. We would like to thank Natalie Stull for mouse islet isolations and Carrie Sedam for technical assistance. Pancreatic human islets were obtained through the Integrated Islet Distribution Program, IIDP. This study was supported by grants from the National Institutes of Health (DK067912 and DK076614 to D.C.T., CTSI-KL2 RR025760 to ZW, and T32 DK064466 and F32 DK094488 to SMY) and the American Heart Association (10PRE3040010 to MAK).

REFERENCES

1. LeRoith, D.; Taylor, SI.; Olefsky, JM. Diabetes mellitus : a fundamental and clinical text. 3rd ed.. Lippincott Williams & Wilkins; Philadelphia: 2004. p. xviiip. 1540
2. Ashcroft FM, Harrison DE, Ashcroft SJ. Glucose induces closure of single potassium channels in isolated rat pancreatic beta-cells. Nature. 1984; 312(5993):446–8. [PubMed: 6095103]
3. Cook DL, Hales CN. Intracellular ATP directly blocks K+ channels in pancreatic B-cells. Nature. 1984; 311(5983):271–3. [PubMed: 6090930]
4. Rorsman P, Ashcroft FM, Trube G. Single Ca channel currents in mouse pancreatic B-cells. Pflugers Arch. 1988; 412(6):597–603. [PubMed: 2463514]
5. Satin LS, Cook DL. Voltage-gated Ca2+ current in pancreatic B-cells. Pflugers Arch. 1985; 404(4): 385–7. [PubMed: 2414720]
6. Orci L, Gabbay KH, Malaisse WJ. Pancreatic beta-cell web: its possible role in insulin secretion. Science. 1972; 175(26):1128–30. [PubMed: 4551150]
7. Cai EP, Casimir M, Schroer SA, Luk CT, Shi SY, Choi D, et al. In Vivo Role of Focal Adhesion Kinase in Regulating Pancreatic beta-Cell Mass and Function Through Insulin Signaling, Actin Dynamics, and Granule Trafficking. Diabetes. 2012; 61(7):1708–18. [PubMed: 22498697]
8. Olofsson CS, Hakansson J, Salehi A, Bengtsson M, Galvanovskis J, Partridge C, et al. Impaired insulin exocytosis in neural cell adhesion molecule-/- mice due to defective reorganization of the submembrane F-actin network. Endocrinology. 2009; 150(7):3067–75. [PubMed: 19213846]

9. Thurmond DC, Gonelle-Gispert C, Furukawa M, Halban PA, Pessin JE. Glucose-Stimulated Insulin Secretion Is Coupled to the Interaction of Actin with the t-SNARE (Target Membrane Soluble N-Ethylmaleimide-Sensitive Factor Attachment Protein Receptor Protein) Complex. Mol Endocrinol. 2003; 17(4):732–42. [PubMed: 12554769]
10. Huang P, Yeku O, Zong H, Tsang P, Su W, Yu X, et al. Phosphatidylinositol-4-phosphate-5-kinase alpha deficiency alters dynamics of glucose-stimulated insulin release to improve glucohomeostasis and decrease obesity in mice. Diabetes. 2011; 60(2):454–63. [PubMed: 21270258]
11. Tomas A, Yermen B, Min L, Pessin JE, Halban PA. Regulation of pancreatic beta-cell insulin secretion by actin cytoskeleton remodelling: role of gelsolin and cooperation with the MAPK signalling pathway. J Cell Sci. 2006; 119(Pt 10):2156–67. [PubMed: 16638805]
12. Kalwat MA, Wiseman DA, Luo W, Wang Z, Thurmond DC. Gelsolin Associates with the N-terminus of Syntaxin 4 to Regulate Insulin Granule Exocytosis. Mol Endocrinol. 2012; 26(1):128–41. [PubMed: 22108804]
13. Rondas D, Tomas A, Soto-Ribeiro M, Wehrle-Haller B, Halban PA. Novel mechanistic link between focal adhesion remodeling and glucose-stimulated insulin secretion. J Biol Chem. 2012; 287(4):2423–36. [PubMed: 22139838]
14. Nevins AK, Thurmond DC. Glucose regulates the cortical actin network through modulation of Cdc42 cycling to stimulate insulin secretion. Am J Physiol Cell Physiol. 2003; 285(3):C698–710. [PubMed: 12760905]
15. Henquin JC. The dual control of insulin secretion by glucose involves triggering and amplifying pathways in beta-cells. Diabetes research and clinical practice. 2011; 93(Suppl 1):S27–31. [PubMed: 21864748]
16. Wang Z, Oh E, Clapp DW, Chernoff J, Thurmond DC. Inhibition or ablation of p21-activated kinase (PAK1) disrupts glucose homeostatic mechanisms in vivo. J Biol Chem. 2011; 286(48): 41359–67. [PubMed: 21969371]
17. Wang Z, Oh E, Thurmond DC. Glucose-stimulated Cdc42 signaling is essential for the second phase of insulin secretion. J Biol Chem. 2007; 282(13):9536–46. [PubMed: 17289663]
18. Kepner EM, Yoder SM, Oh E, Kalwat MA, Wang Z, Quilliam LA, et al. Cool-1/betaPIX functions as a guanine nucleotide exchange factor in the cycling of Cdc42 to regulate insulin secretion. Am J Physiol Endocrinol Metab. 2011; 301(6):E1072–80. [PubMed: 21828338]
19. Shibasaki TUE, Takahashi H, Hamaguchi H, Tatebe M, Oiso Y, Seino S. Role of Cdc42/N-WASP Signaling-Regulated Actin Dynamics in Insulin Secretion. Diabetes. 2011; 60(Supplement 1):A542.
20. Kowluru A, Li G, Rabaglia ME, Segu VB, Hofmann F, Aktories K, et al. Evidence for differential roles of the Rho subfamily of GTP-binding proteins in glucose- and calcium-induced insulin secretion from pancreatic beta cells. Biochem Pharmacol. 1997; 54(10):1097–108. [PubMed: 9464452]
21. Li J, Luo R, Kowluru A, Li G. Novel regulation by Rac1 of glucose- and forskolin-induced insulin secretion in INS-1 beta-cells. Am J Physiol Endocrinol Metab. 2004; 286(5):E818–27. [PubMed: 14736704]
22. Edwards DC, Sanders LC, Bokoch GM, Gill GN. Activation of LIM-kinase by Pak1 couples Rac/Cdc42 GTPase signalling to actin cytoskeletal dynamics. Nature Cell Biol. 1999; 1(5):253–9. [PubMed: 10559936]
23. Vadlamudi RK, Li F, Adam L, Nguyen D, Ohta Y, Stossel TP, et al. Filamin is essential in actin cytoskeletal assembly mediated by p21-activated kinase 1. Nature Cell Biol. 2002; 4(9):681–90. [PubMed: 12198493]
24. Vadlamudi RK, Li F, Barnes CJ, Bagheri-Yarmand R, Kumar R. p41-Arc subunit of human Arp2/3 complex is a p21-activated kinase-1-interacting substrate. EMBO reports. 2004; 5(2):154–60. [PubMed: 14749719]
25. Sanders LC, Matsumura F, Bokoch GM, de Lanerolle P. Inhibition of myosin light chain kinase by p21-activated kinase. Science. 1999; 283(5410):2083–5. [PubMed: 10092231]
26. Park ER, Eblen ST, Catling AD. MEK1 activation by PAK: a novel mechanism. Cellular signalling. 2007; 19(7):1488–96. [PubMed: 17314031]

27. Coles LC, Shaw PE. PAK1 primes MEK1 for phosphorylation by Raf-1 kinase during cross-cascade activation of the ERK pathway. Oncogene. 2002; 21(14):2236–44. [PubMed: 11948406]
28. Silander K, Scott LJ, Valle TT, Mohlke KL, Stringham HM, Wiles KR, et al. A large set of Finnish affected sibling pair families with type 2 diabetes suggests susceptibility loci on chromosomes 6, 11, and 14. Diabetes. 2004; 53(3):821–9. [PubMed: 14988269]
29. Palmer ND, Langefeld CD, Campbell JK, Williams AH, Saad M, Norris JM, et al. Genetic mapping of disposition index and acute insulin response loci on chromosome 11q. The Insulin Resistance Atherosclerosis Study (IRAS) Family Study. Diabetes. 2006; 55(4):911–8. [PubMed: 16567510]
30. Lopez JP, Turner JR, Philipson LH. Glucose-induced ERM protein activation and translocation regulates insulin secretion. Am J Physiol Endocrinol Metab. 2010; 299(5):E772–85. [PubMed: 20739507]
31. Ke B, Oh E, Thurmond DC. Doc2beta is a novel Munc18c-interacting partner and positive effector of syntaxin 4-mediated exocytosis. J Biol Chem. 2007; 282(30):21786–97. [PubMed: 17548353]
32. Deacon SW, Beeser A, Fukui JA, Rennefahrt UE, Myers C, Chernoff J, et al. An isoform-selective, small-molecule inhibitor targets the autoregulatory mechanism of p21-activated kinase. Chem Biol. 2008; 15(4):322–31. [PubMed: 18420139]
33. Viaud J, Peterson JR. An allosteric kinase inhibitor binds the p21-activated kinase autoregulatory domain covalently. Mol Cancer Ther. 2009; 8(9):2559–65. [PubMed: 19723886]
34. Nevins AK, Thurmond DC. A direct interaction between Cdc42 and vesicle-associated membrane protein 2 regulates SNARE-dependent insulin exocytosis. J Biol Chem. 2005; 280(3):1944–52. [PubMed: 15537656]
35. Riedl J, Crevenna AH, Kessenbrock K, Yu JH, Neukirchen D, Bista M, et al. Lifeact: a versatile marker to visualize F-actin. Nat Methods. 2008; 5(7):605–7. [PubMed: 18536722]
36. Rondas D, Tomas A, Halban PA. Focal adhesion remodeling is crucial for glucose-stimulated insulin secretion and involves activation of focal adhesion kinase and paxillin. Diabetes. 2011; 60(4):1146–57. [PubMed: 21357465]
37. Kowluru A, Veluthakal R, Rhodes CJ, Kamath V, Syed I, Koch BJ. Protein farnesylation-dependent Raf/extracellular signal-related kinase signaling links to cytoskeletal remodeling to facilitate glucose-induced insulin secretion in pancreatic beta-cells. Diabetes. 2010; 59(4):967–77. [PubMed: 20071600]
38. Alejandro EU, Lim GE, Mehran AE, Hu X, Taghizadeh F, Pelipeychenko D, et al. Pancreatic {beta}-cell Raf-1 is required for glucose tolerance, insulin secretion, and insulin 2 transcription. FASEB J. 2011; 25(11):3884–95. [PubMed: 21817126]
39. Surviladze, Z.; Waller, A.; Strouse, JJ.; Bologa, C.; Ursu, O.; Salas, V., et al. Probe Reports from the NIH Molecular Libraries Program. Bethesda (MD): 2010. A Potent and Selective Inhibitor of Cdc42 GTPase..
40. Bain J, Plater L, Elliott M, Shpiro N, Hastie CJ, McLauchlan H, et al. The selectivity of protein kinase inhibitors: a further update. Biochem J. 2007; 408(3):297–315. [PubMed: 17850214]
41. Henquin JC. Triggering and amplifying pathways of regulation of insulin secretion by glucose. Diabetes. 2000; 49(11):1751–60. [PubMed: 11078440]
42. Bratanova-Tochkova TK, Cheng H, Daniel S, Gunawardana S, Liu YJ, Mulvaney-Musa J, et al. Triggering and augmentation mechanisms, granule pools, and biphasic insulin secretion. Diabetes. 2002; 51(Suppl 1):S83–90. [PubMed: 11815463]
43. Straub SG, Sharp GW. Glucose-stimulated signaling pathways in biphasic insulin secretion. Diabetes Metabolism Res Rev. 2002; 18(6):451–63.
44. Ohara-Imaizumi M, Nakamichi Y, Tanaka T, Ishida H, Nagamatsu S. Imaging exocytosis of single insulin secretory granules with evanescent wave microscopy: distinct behavior of granule motion in biphasic insulin release. J Biol Chem. 2002; 277(6):3805–8. [PubMed: 11751926]
45. Regazzi R, Wollheim CB, Lang J, Theler JM, Rossetto O, Montecucco C, et al. VAMP-2 and cellubrevin are expressed in pancreatic beta-cells and are essential for Ca(2+)-but not for GTP gamma S-induced insulin secretion. EMBO J. 1995; 14(12):2723–30. [PubMed: 7796801]

46. Muriel O, Echarri A, Hellriegel C, Pavon DM, Beccari L, Del Pozo MA. Phosphorylated filamin A regulates actin-linked caveolae dynamics. J Cell Sci. 2011; 124(Pt 16):2763–76. [PubMed: 21807941]
47. Tan JL, Ravid S, Spudich JA. Control of nonmuscle myosins by phosphorylation. Ann Rev Biochem. 1992; 61:721–59. [PubMed: 1497323]
48. Yu W, Niwa T, Fukasawa T, Hidaka H, Senda T, Sasaki Y, et al. Synergism of protein kinase A, protein kinase C, and myosin light-chain kinase in the secretory cascade of the pancreatic beta-cell. Diabetes. 2000; 49(6):945–52. [PubMed: 10866046]
49. Wilson JR, Ludowyke RI, Biden TJ. A redistribution of actin and myosin IIA accompanies Ca(2+)-dependent insulin secretion. FEBS Lett. 2001; 492(1-2):101–6. [PubMed: 11248245]
50. Wilson JR, Biden TJ, Ludowyke RI. Increases in phosphorylation of the myosin II heavy chain, but not regulatory light chains, correlate with insulin secretion in rat pancreatic islets and RINm5F cells. Diabetes. 1999; 48(12):2383–9. [PubMed: 10580427]
51. Klemke RL, Cai S, Giannini AL, Gallagher PJ, de Lanerolle P, Cheresh DA. Regulation of cell motility by mitogen-activated protein kinase. J Cell Biol. 1997; 137(2):481–92. [PubMed: 9128257]
52. Longuet C, Broca C, Costes S, Hani EH, Bataille D, Dalle S. Extracellularly regulated kinases 1/2 (p44/42 mitogen-activated protein kinases) phosphorylate synapsin I and regulate insulin secretion in the MIN6 beta-cell line and islets of Langerhans. Endocrinology. 2005; 146(2):643–54. [PubMed: 15498890]
53. Jacobo SM, Guerra ML, Hockerman GH. Cav1.2 and Cav1.3 are differentially coupled to glucagon-like peptide-1 potentiation of glucose-stimulated insulin secretion in the pancreatic beta-cell line INS-1. J Pharmacol Exp Ther. 2009; 331(2):724–32. [PubMed: 19710366]
54. Briaud I, Lingohr MK, Dickson LM, Wrede CE, Rhodes CJ. Differential activation mechanisms of Erk-1/2 and p70(S6K) by glucose in pancreatic beta-cells. Diabetes. 2003; 52(4):974–83. [PubMed: 12663469]
55. Nie J, Sun C, Faruque O, Ye G, Li J, Liang Q, et al. Synapses of amphids defective (SAD-A) kinase promotes glucose-stimulated insulin secretion through activation of p21-activated kinase (PAK1) in pancreatic beta-cells. J Biol Chem. 2012; 287(31):26435–44. [PubMed: 22669945]
56. Gromada J, Brock B, Schmitz O, Rorsman P. Glucagon-like peptide-1: regulation of insulin secretion and therapeutic potential. Bas Clin Pharm Tox. 2004; 95(6):252–62.
57. Arnette D, Gibson TB, Lawrence MC, January B, Khoo S, McGlynn K, et al. Regulation of ERK1 and ERK2 by glucose and peptide hormones in pancreatic beta cells. J Biol Chem. 2003; 278(35): 32517–25. [PubMed: 12783880]
58. Khoo S, Griffen SC, Xia Y, Baer RJ, German MS, Cobb MH. Regulation of insulin gene transcription by ERK1 and ERK2 in pancreatic beta cells. J Biol Chem. 2003; 278(35):32969–77. [PubMed: 12810726]
59. Lim GE, Xu M, Sun J, Jin T, Brubaker PL. The Rho Guanosine 5'-Triphosphatase, Cell Division Cycle 42, Is Required for Insulin-Induced Actin Remodeling and Glucagon-Like Peptide-1 Secretion in the Intestinal Endocrine L Cell. Endocrinology. 2009; 150(12):5249–61. [PubMed: 19819966]

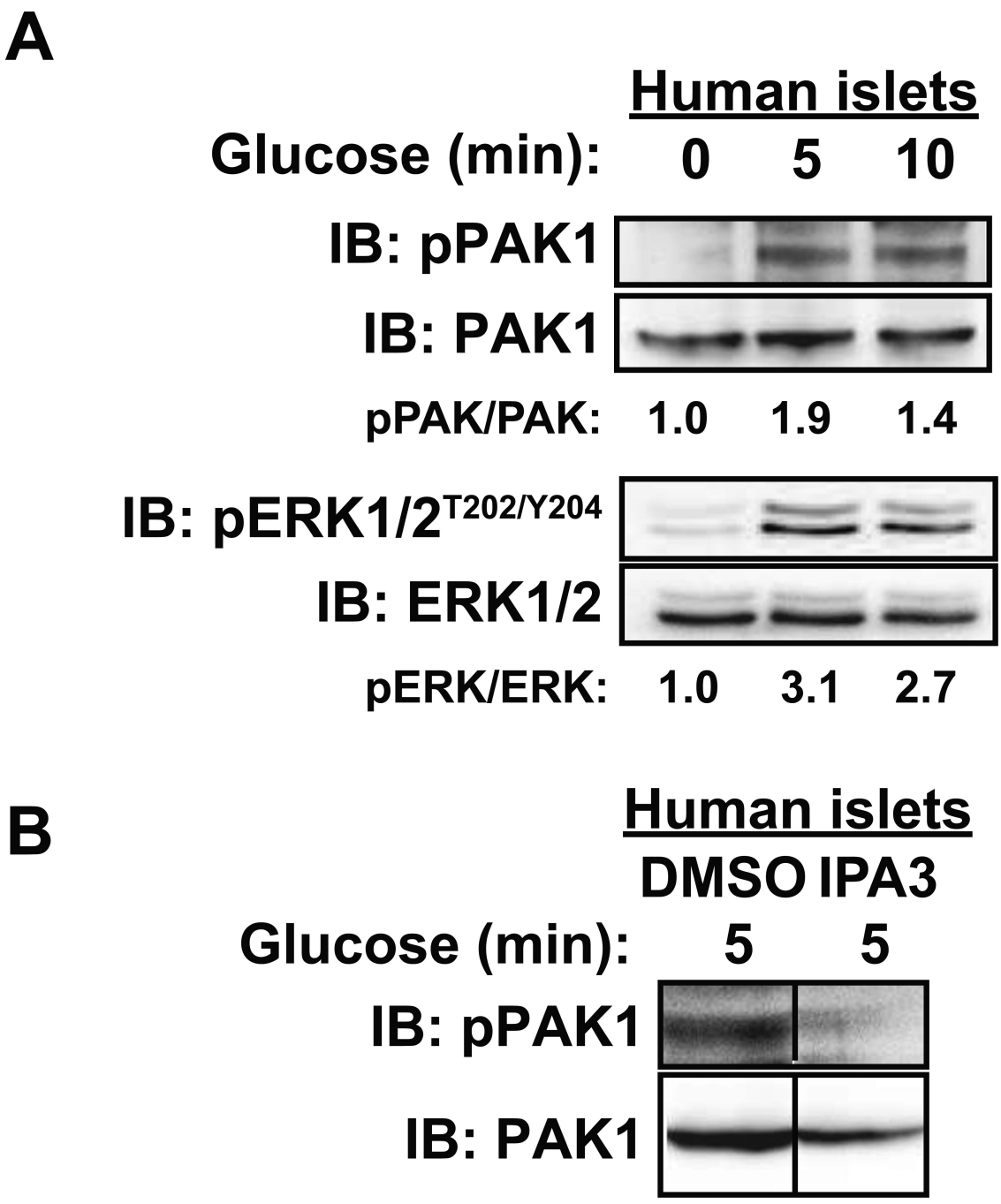

Figure 1. In human islets, glucose-stimulated PAK1 activation and downstream signaling is prevented by IPA3

A) Human islets were incubated in KRBH with 2.8 mM glucose for 2 h and then stimulated with 16.7 mM glucose for 0, 5 or 10 min. Islets were lysed for SDS-PAGE and immunoblotting (*IB*) for phosphorylated (pPAK1) and total PAK1 and ERK1/2 protein abundances. Optical density scanning was used to quantify three different batches of human donor islets, with averages of the proportion of pPAK1/total PAK1; phosphorylated ERK1/2 (pERK1/2)/total ERK1/2 is shown below each lane; $P<0.05$, *versus* unstimulated cells. Data are representative of three sets of human donor islets. ***B)*** Human islets were incubated overnight in CMRL with containing either vehicle (DMSO) or low-dosage IPA3 (7.5 μM)

as described previously (16). Islets were then incubated in KRBH with 2.8 mM glucose for 2 h, still in the presence of vehicle or IPA3, and then stimulated with 16.7 mM glucose for 5 min before harvest for SDS-PAGE and immunoblotting for phosphorylated (pPAK1) and total PAK1. Data are representative of two sets of human donor islets. Vertical lines denote splicing of lanes from within the same gel exposure.

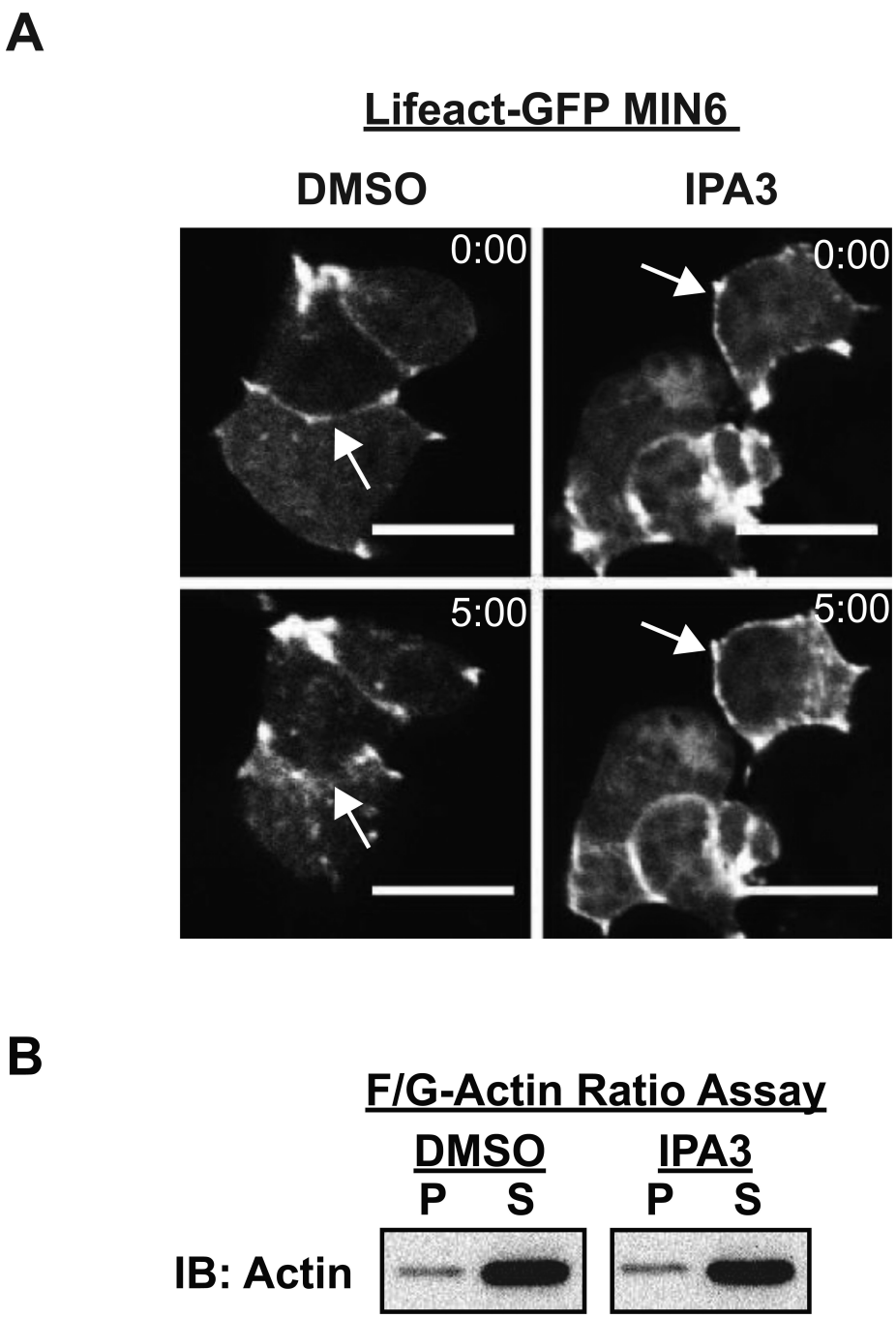

Figure 2. PAK1 activity is required for glucose-stimulated cortical F-actin remodeling, as determined using live-cell imaging of Lifeact-GFP expressing MIN6 β cells

A) MIN6 cells were transfected with Lifeact-GFP plasmid DNA and incubated 48 h to allow protein expression. Lifeact-GFP expressing cells were then preincubated for 2 h in MKRBB, and either vehicle (DMSO) or 30 μM IPA3 was added to the buffer 10 min before live-cell confocal imaging. Images were collected every minute for 5 min. Representative images of 11 cells from 3 independent experiments assessing basal (0:00) and glucose (20 mM)-stimulated (5:00) Lifeact-GFP are shown. *Scale bar*, 10 μm. ***B)*** MIN6 cells were preincubated in MKRBB for 2 h followed by a 10 min pretreatment with either DMSO or 30 μM IPA3. Cells were then harvested for F:G-Actin ratio analysis. Supernatant (S) and pellet

(P) fractions containing G-actin and F-actin, respectively, prepared from unstimulated cells were subjected to SDS-PAGE for immunoblotting (*IB*). Glucose-stimulated (5 min) ratios were similar to the unstimulated ratios (data not shown). Data shown are representative of three independent experiments.

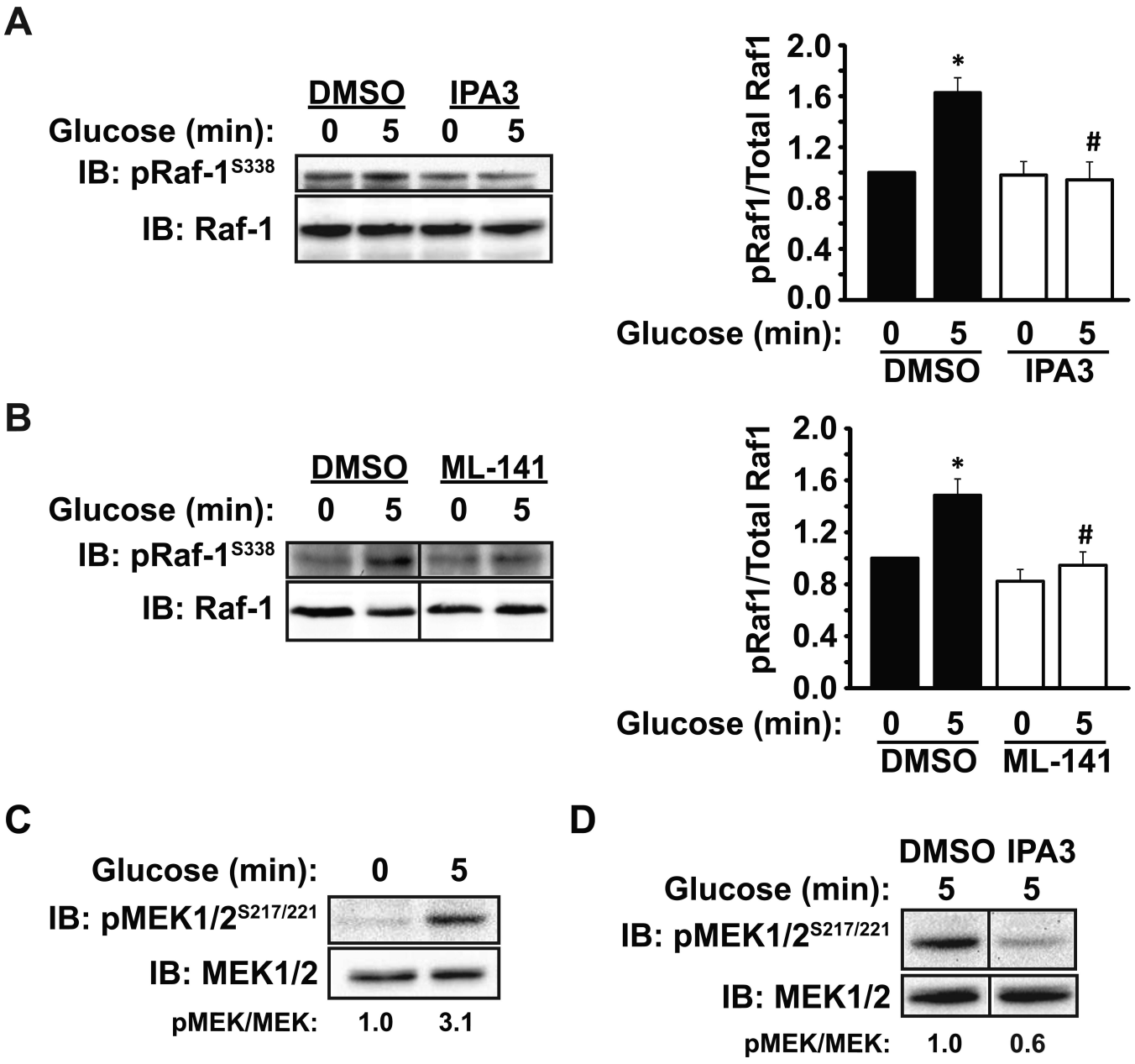

Figure 3. Cdc42 and PAK1 signaling event requirements for activation of Raf-1 and MEK1/2 in MIN6 β cells

A) MIN6 cells were preincubated for 2 h in MKRBB, and either vehicle (DMSO) or 30 μM IPA3 was added to the buffer 10 min before glucose stimulation and harvesting for SDS-PAGE and immunoblot (*IB*) analysis. Bar graph quantitation of at least three independent experiments is shown to the right of the blots; **P<0.05*, versus vehicle basal; #*P<0.05*, versus vehicle stimulated. ***B)*** MIN6 cells were preincubated for 1 h in MKRBB, and either vehicle (DMSO) or 20 μM ML-141 was added to the buffer 1 h before glucose stimulation and harvesting for SDS-PAGE and immunoblot (*IB*) analysis. Bar graph quantitation of at least three independent experiments is shown to the right of the blots; **P<0.05*, versus vehicle basal; #*P<0.05*, versus vehicle stimulated. ***C)*** MIN6 cells were preincubated for 2 h in MKRBB before stimulation with 20 mM glucose. Detergent whole cell lysates were collected and subjected to SDS-PAGE analysis and immunoblotting with antibodies to

phosphorylated and total MEK1/2. Optical density scanning was used to quantify three independent sets of lysates, with averages of the proportion of phosphorylated MEK1/2 (pMEK1/2)/total MEK1/2 shown below each lane, with each set first normalized to fold over basal (1.0). ***D)*** MIN6 cells were treated as in (C) except the MKRBB contained either vehicle or 30 μM IPA3 for 10 min prior to the 5 min glucose before stimulation. Percentages below the lanes denote the average ratio of pMEK1/2/total MEK1/2 in three independent experiments; $P<0.01$). Vertical lines denote splicing of lanes from within the same gel exposure.

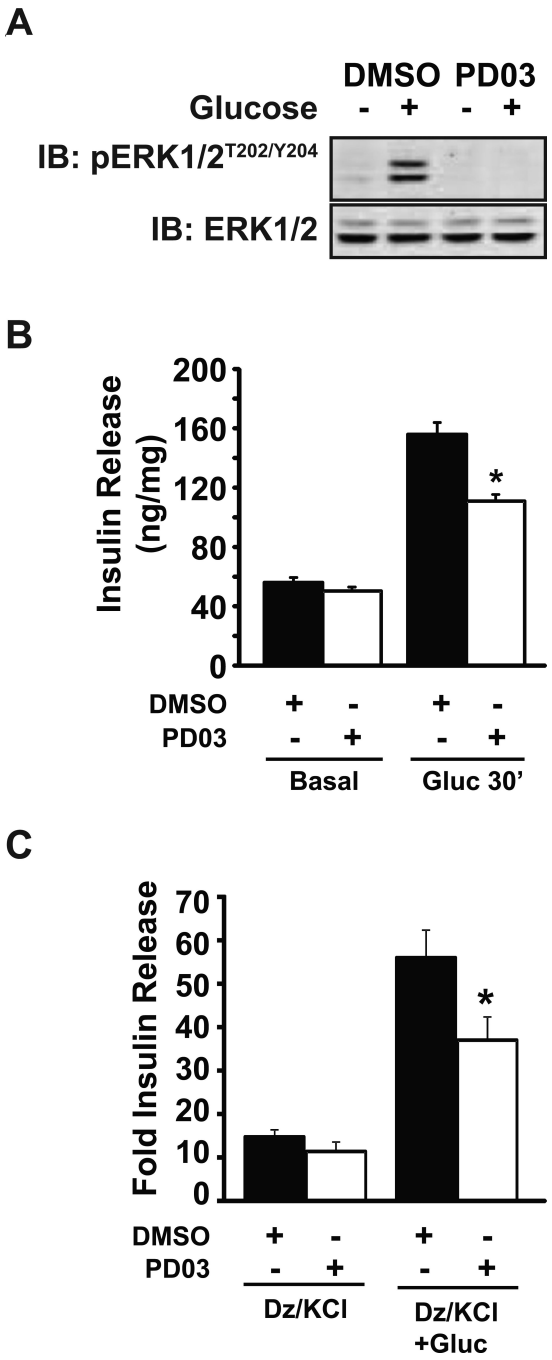

Figure 4. ERK1/2 signaling contributes to the amplification/sustained phase of insulin release

A) MIN6 cells were preincubated for 1 h in MKRBB, and either vehicle (DMSO) or 1 μM PD03 was added to the buffer for 1 h prior to stimulation with 20 mM glucose for 30 min. Lysates were subjected to SDS-PAGE and immunoblotting (*IB*) for phosphorylated and total ERK1/2. Data are representative of three independent experiments. ***B)*** Insulin secreted into the buffer in (A) was quantified by RIA and normalized for protein content corresponding to each accompanying cell lysate; **P*<0.05, *versus* glucose-stimulated vehicle. ***C)*** MIN6 cells treated as described for (A) were exposed to 250 μM diazoxide (Dz) for 10 min before stimulation with 35 mM KCl (Dz/KCl) or 35 mM KCl plus 20 mM glucose (Dz/KCl+Gluc)

for 30 min. Supernatants were collected for insulin radioimmunoassay. Insulin secreted in three independent experiments was quantified by RIA and normalized for protein content corresponding to each accompanying cell lysate. Data are shown as the stimulation index (SI=stimulated insulin release/unstimulated) for each independent experiment; $*P<0.05$, *versus* glucose-stimulated vehicle cells.

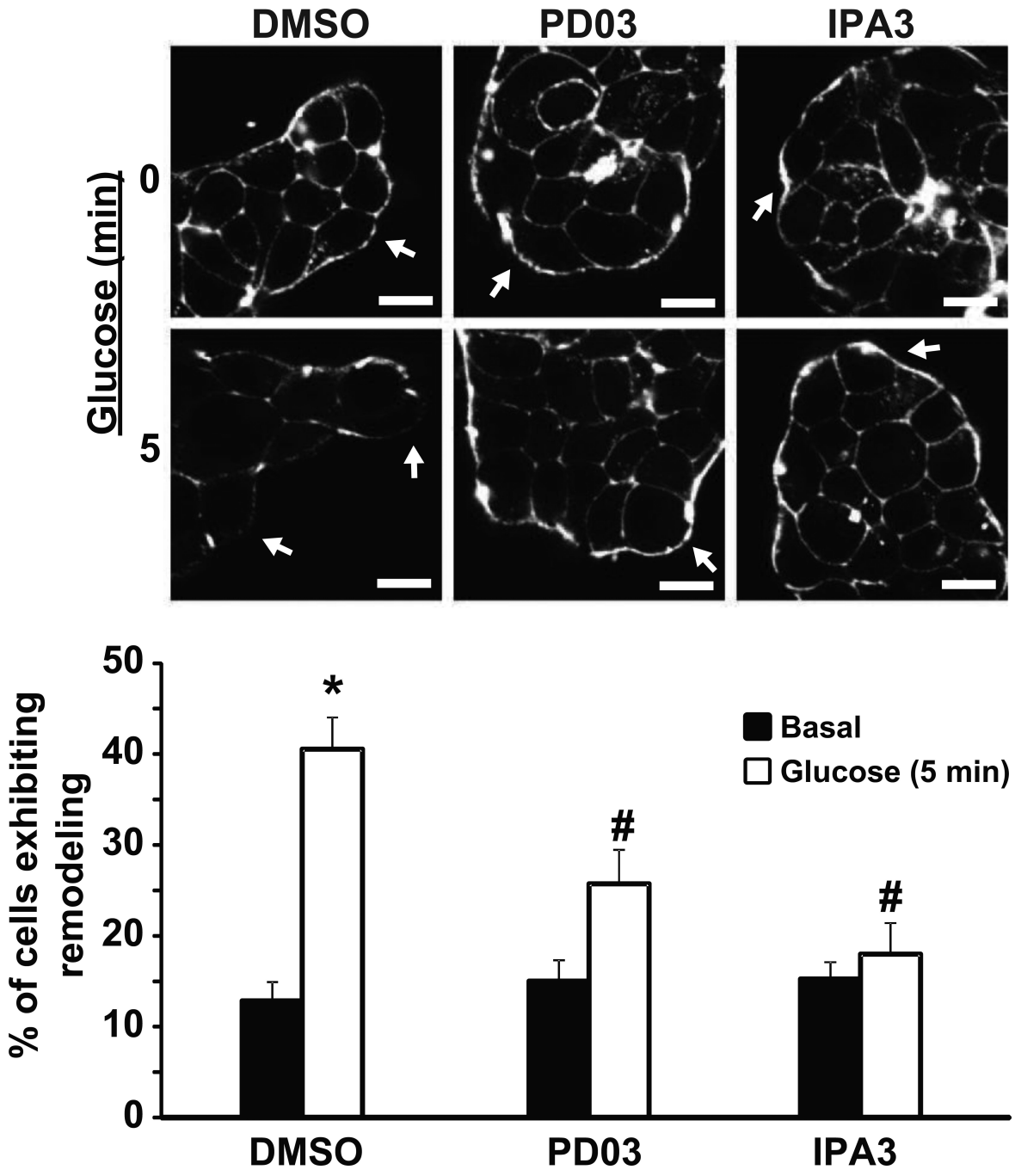

Figure 5. ERK1/2 activation is required for glucose-induced cortical F-actin remodeling in MIN6 β cells

MIN6 cells plated on glass cover slides were pre-incubated in MKRBB for 2 h and left unstimulated (top images) or stimulated with 20 mM glucose for 5 min (bottom images). Cells were fixed, permeabilized and cortical F-actin changes monitored by Rhodamine-Phalloidin staining. Cells were imaged at the midplane by single channel scanning confocal microscopy to determine F-actin remodeling. Arrows indicate cortical regions of MIN6 cells. *Scale bar*, 10 μm. Bar graph represents the average percentage of cells exhibiting F-actin remodeling ± S.E. of three independent experiments, where each experiment contained 6 to 12 fields (number of cells examined per condition: DMSO basal=195, DMSO

Glucose=173, PD03 basal=122, PD03 Glucose=183, IPA3 basal=116 cells, IPA3 Glucose=108); *P<0.05, *versus* unstimulated vehicle cells, $^{\#}P$<0.05, *versus* stimulated vehicle cells. Statistical analysis was performed by one-way ANOVA using multiple comparisons.

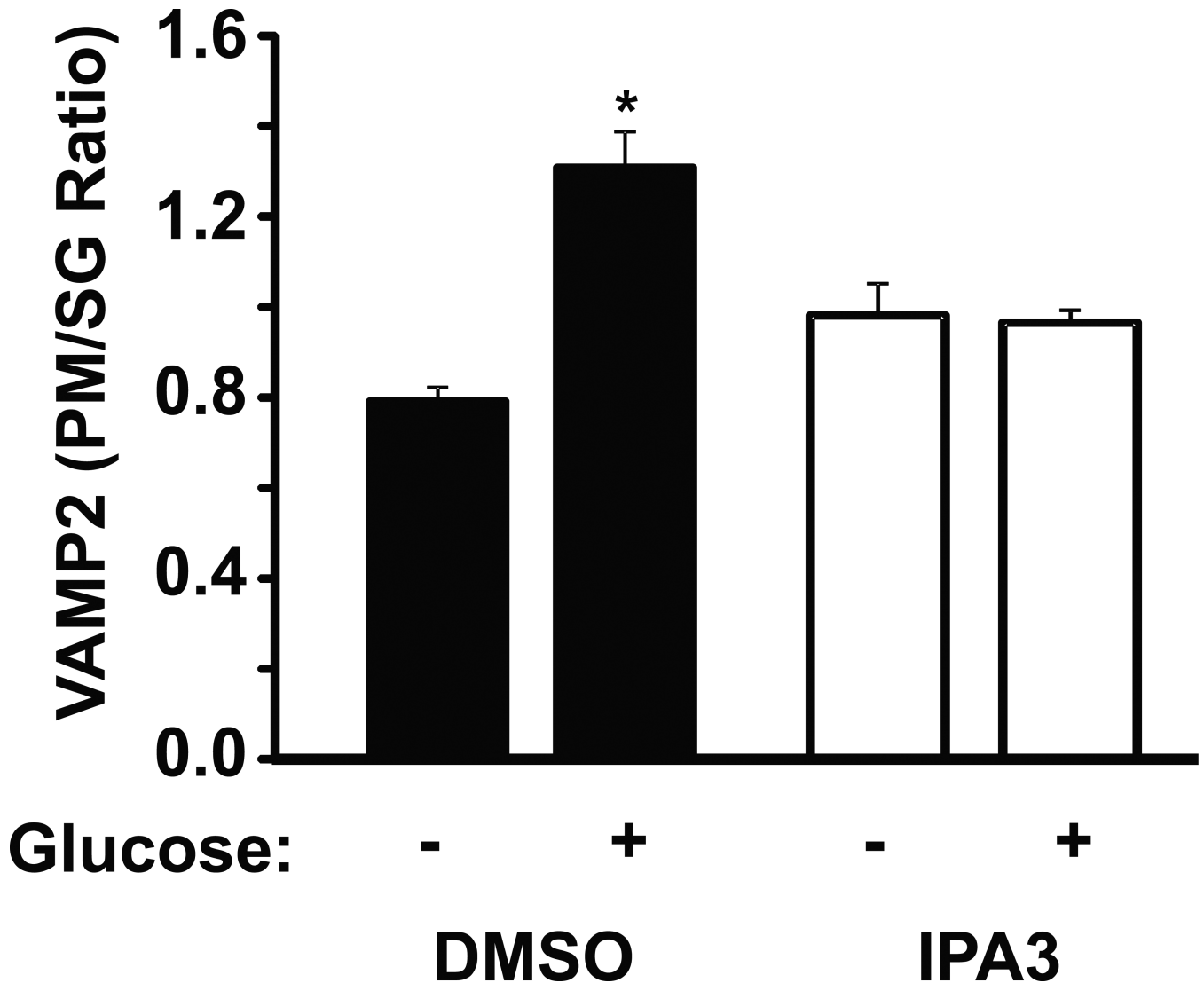

Figure 6. PAK1 is required for glucose-stimulated insulin granule accumulation at the β cell plasma membrane

MIN6 cells were preincubated for 2 h in MKRBB and either vehicle (DMSO) or 30 μM IPA3 was added 10 min prior to stimulation with 20 mM glucose for 20 min. Cells were harvested and subjected to subcellular fractionation. Isolated plasma membrane (PM) and secretory granule (SG) fractions were analyzed by SDS-PAGE and immunoblotting (*IB*) for the granule v-SNARE and marker protein VAMP2. Optical density quantitation of VAMP2 in the PM versus the SG for each of three independent sets of fractions yielded the VAMP2 PM/SG ratio, represented in the bar graph as the average ± S.E.; **P*<0.05, *versus* unstimulated vehicle fractions).

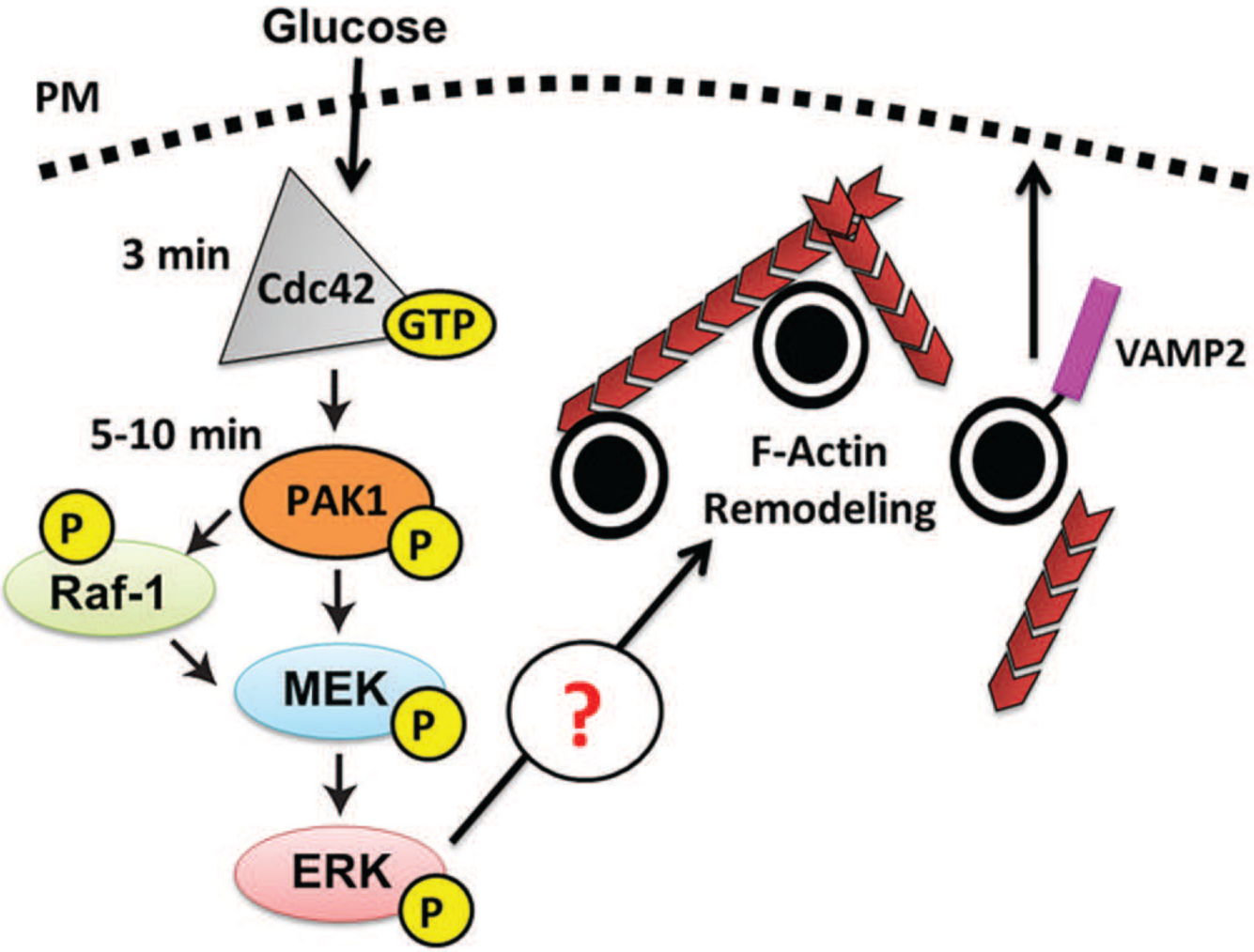

Figure 7. Model of Cdc42-PAK1 signaling in the β cell

Glucose enters the β cell, activating Cdc42, then PAK1. Cdc42→PAK1 signaling activates Raf-1 and MEK1/2, which induces ERK1/2 activation. This glucose-stimulated signaling cascade culminating in ERK1/2 activation induces F-actin remodeling, insulin granule accumulation/recruitment to the plasma membrane, events required for the amplification/sustained phase of insulin secretion.